Chapter

Pulsed Laser Deposition of Transition Metal Dichalcogenides-Based Heterostructures for Efficient Photodetection

Deependra Kumar Singh, Karuna Kar Nanda and Saluru Baba Krupanidhi

Abstract

From the past few decades, photodetectors (PDs) are being regarded as crucial components of many photonic devices which are being used in various important applications. However, the PDs based on the traditional bulk semiconductors still face a lot of challenges as far as the device performance is concerned. To overcome these limitations, a novel class of two-dimensional materials known as transition metal dichalcogenides (TMDCs) has shown great promise. The TMDCs-based PDs have been reported to exhibit competitive figures of merit to the state-of-the-art PDs, however, their production is still limited to laboratory scale due to limitations in the conventional fabrication methods. Compared to these traditional synthesis approaches, the technique of pulsed laser deposition (PLD) offers several merits. PLD is a physical vapor deposition approach, which is performed in an ultrahigh-vacuum environment. Therefore, the products are expected to be clean and free from contaminants. Most importantly, PLD enables actualization of large-area thin films, which can have a significant potential in the modern semiconductor industry. In the current chapter, the growth of TMDCs by PLD for applications in photodetection has been discussed, with a detailed analysis on the recent advancements in this area. The chapter will be concluded by providing an outlook and perspective on the strategies to overcome the shortcomings associated with the current devices.

Keywords: two-dimensional semiconductors, transition metal dichalcogenides, pulsed laser deposition, photodetectors

1. Introduction

Photodetectors (PDs) are the optoelectronic devices which convert incident optical signals into electrical outputs through the phenomenon of light-matter interaction, which can be processed by the conventional read-out electronics. PDs form the basis of many vital components present in numerous electronic and optoelectronic devices as they find applications in a broad range of fields such as

in photovoltaics [1, 2], military and defense technology [3], optical communication [4], remote sensing [3], biomedical imaging [5], environmental and ozone layer monitoring [4], and so on. Therefore, highly efficient photodetection has become very crucial for the industrial and scientific communities. With advancements in the matured technology of three-dimensional (3D) semiconductors [6–17] such as gallium nitride (GaN), zinc oxide (ZnO), indium gallium nitride (InGaN), indium nitride (InN), gallium oxide (Ga_2O_3), gallium arsenide (GaAs), silicon (Si), aluminum gallium nitride (AlGaN), germanium (Ge), mercury cadmium telluride (HgCdTe), gallium antimonide (GaSb), and so forth, high-performance PDs sensitive to wavelengths in the entire ultraviolet (UV)-far infrared (FIR) have been successfully fabricated. However, further advances in these PDs are hindered by the certain drawbacks encountered due to the intrinsic limitations in 3D semiconductors such as lower charge carrier mobilities, low light absorption properties, presence of dangling bonds at the interface, high fabrication costs involved, and so forth [18]. Thus, it is crucial to explore alternate materials, which can overcome the above-mentioned drawbacks for the development of multifunctional PDs.

The successful delamination of graphene in the revolutionary work by Geim and Novoselov in 2004 [19] ignited a plethora of research, in the field of two-dimensional (2D) layered materials and their heterostructures [20–22]. In the recent years, the amount of research focused on these layered materials has increased multifold. A layered material is nothing but an ultrathin phase of a material, scaled down to the level of atomic thickness, and is characterized by weak inter-layer van der Waals (vdW) forces and a strong intra-layer covalent interaction [23]. This makes these ultrathin materials possess electronic and optoelectronic properties such as band gap, mobility, etc., that are thickness-dependent [24], and thus, their novel chemical and physical characteristics pave a way towards the unexplored areas, both in the fields of fundamental research as well as engineering applications. In spite of possessing unparalleled electronic and optoelectronic properties such as high carrier mobility, dangling bonds-free surface, large current carrying capacities, excellent mechanical properties, the zero band gap or the gapless electronic structure of graphene [25] limits its use in realization of practical applications-based PDs, which demand switching behavior or in other words, a definite on/off state. This has led to the exploration of graphene alternatives with a substantial band gap, and researchers and scientists across the world have resurrected a class of conventional 2D materials known as the transition metal dichalcogenides (TMDCs), characterized by low-fabrication cost, chemical stability, earth-abundance and environment-friendly properties. Some of the well-studied TMDCs are molybdenum disulfide (MoS_2), tungsten disulfide (WS_2), molybdenum diselenide ($MoSe_2$), molybdenum ditelluride ($MoTe_2$), tungsten diselenide (WSe_2), and so on [26–28]. As of now, semiconductors of the TMDC family have enabled tremendous accomplishments in the field of photodetection, such as from monofunctional to multifunctional PDs, from homogeneous to hybrid 2D semiconductors-based PDs, and from rigid to flexible electronic devices [29–31].

Regardless of the efforts of the researchers and scientists, some common challenges are still being faced related to fabrication and the performance of these TMDCs-based devices [18]. The challenges include growth of high-quality crystals, controlling the morphology and the thickness, scaling up the growth for industrial scale production, optimizing the device architectures, and so forth. To address these challenges, pulsed laser deposition (PLD) has emerged as a perfect tool for the synthesis of TMDCs. With the use of PLD, the actualization of high quality and wafer scale synthesis of TMDCs has become possible [32]. Eminently, PDs based on the PLD-synthesized TMDCs have exhibited competitive device performance

parameters when compared with the commercial PDs, and thus, offer great opportunities towards the next generation photonics. In the subsequent section, we will give an introduction about TMDCs and their properties. Afterwards, the fundamentals of PLD will be discussed in detail, followed by the recent advancements in the PLD-grown TMDCs for photodetection application. Finally, we will conclude by highlighting the unresolved problems and suggest future perspectives in this evolving field of optoelectronics.

2. Transition metal dichalcogenides (TMDCs)

TMDCs are denoted by the general formula of MX_2 where M and X represent a transition metal (Mo, Nb, W, Hf, Ti, and so on), and a chalcogen (S, Te, and Se), respectively. In the periodic table, groups IV-X belong to the transition metals and they contain different number of d-electrons. Thus, the difference in the valance d-electrons of different transition metals gives rise to the different electronic properties such as metallic, semiconducting, and superconducting [33]. TMDCs exist in a layered form at the atomic level, containing one or few monolayers. **Figure 1(a)** shows a schematic depicting the layered structure of MoS_2.

A TMDC can exist in various structural phases which are a result of the different co-ordinations of the transition metal atom. The most common structural phases in which the TMDCs crystallize are the trigonal prismatic (2H) and the octahedral (1T) phase. These crystal phases can also be seen in the terms of different stacking sequences of the atoms (as a representative result, **Figure 1(b)** shows crystal structure of MoS_2). The three atomic planes i.e. chalcogen– metal–chalcogen form the individual layers of TMDCs. The 2H phase corresponds to an ABA stacking, whereas, the 1T phase is characterized by an ABC stacking order. For most of the bulk TMDCs (MoS_2, $MoSe_2$, $MoTe_2$, WS_2, WSe_2, etc.), the 2H phase is thermodynamically more stable than the metastable 1T phase. Tungsten ditelluride (WTe_2) shows an exception where the most stable phase is the orthorhombic ($1T_d$ phase) at room temperature [33].

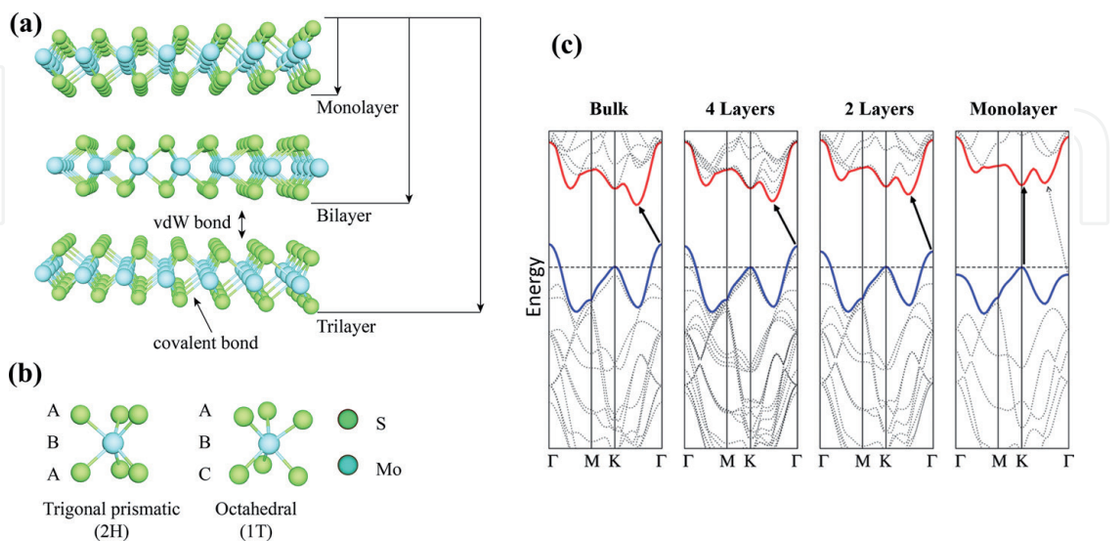

Figure 1.
(a) Schematic showing a monolayer of a TMDC, where the atoms of transition metal are bonded through covalent bonds with the chalcogen atoms. These individual monolayers are stacked and held together by vdW forces to form the bulk structures. (b) Crystal structures of layered MoS_2 with different stacking sequences as shown to form the two most common phases: trigonal prismatic (2H) and octahedral (1T). Figure is adapted from Ref. [23]. (c) Transformation of the band structure of 2H phase of MoS_2 calculated by first principles from bulk to a single layer. Figure is adapted and reproduced with permission from Ref. [34].

The assortment of chemical compositions as well as the different crystal structures of TMDCs results in varying band structure characters, which in turn lead to a wide range of electronic properties. In the thermodynamically most stable 2H phase, MoS_2, WS_2, $MoSe_2$, and WSe_2 show semiconducting behavior [33]. These semiconducting properties accentuated these TMDCs as potential 2D materials for next generation electronic devices. As a representative result, the basic characteristics of the band structure of MoS_2 has been shown in **Figure 1(c)**. The transformation of the band structure as calculated from density functional theory (DFT) for 2H-MoS_2 upon increasing its thickness from monolayer form to the bulk has been shown in **Figure 1(c)**. The positions of the conduction and valence band edges change with increasing the number of layers of MoS_2, and the direct band gap in the monolayer form changes into an indirect band gap in the bulk material [33]. The calculated value of the band gap of the monolayer 2H-MoS_2 is ~1.89 eV [35]. The experimentally observed value for the electronic band gap of 2H-MoS_2 in its monolayer form is 2.15 eV [36]. Notably, the conduction band minimum and the valence band maximum are situated at the two inequivalent high-symmetry points, which represent the corners of the hexagonal Brillouin zone [33]. This attribute is common between monolayer 2H phase MoS_2 (and the other group VI single-layer 2H phase TMDCs) and graphene and allows the observation of potential valleytronics applications.

Through the persistent efforts over the last decade, researchers have developed several techniques to produce ultrathin TMDCs. In principle, these techniques can be broadly classified into two categories. The first one is to produce TMDCs by thinning bulk crystals, which is called as a top-down technique. Different types of exfoliations (mechanical, chemical, etc.) fall under this category. Since different layers of 2D materials are held together by vdW interactions, therefore, the interlayer bonding is weak. Thus, under any external perturbations, bulk 2D materials are readily processed into their few-layered forms. The second category is to produce TMDCs through a bottom-up approach, where constituent atoms and molecules are assembled together to form continuous layers. These mainly include chemical vapor deposition (CVD), atomic layer deposition (ALD), magnetron sputtering, molecular beam epitaxy (MBE) and PLD.

As mentioned above, researchers have developed several methods to fabricate TMDCs. In spite of the substantial progress, none of the above techniques can meet the comprehensive demands for industrial-scale production, as in the terms of process simplicity, good scalability, excellent homogeneity and continuity, high quality of the products, high compositional and thickness control, low cost for mass production and higher safety. The techniques such as exfoliation, CVD and ALD suffer from a huge drawback that the growth process occurs in absence of high vacuum, which generally leads to unclean interfaces, and therefore, one has to compromise with the device performance. Moreover, exfoliation and CVD are further associated with low product yield as the films formed are non-continuous and in the range of several microns. Sputtering and MBE are much more sophisticated in terms of the interface quality due to the involvement of ultrahigh vacuum, however, sputtering is characterized by poor surface quality of the films whereas MBE poses drawbacks such as bulky and expensive setups, time-consuming growths, and limitations in terms of substrates. Such limitations further hinder the utilization of these growth methods for industrial scale fabrication of devices. Thus, research and development towards a potentially competent approach which can address the above issues is greatly required.

PLD is a synthesis technique where a high-power pulsed laser beam is focused on a target, which results in the vaporization of the material in the form of a plasma plume and this material gets deposited on a substrate in the form of a thin film.

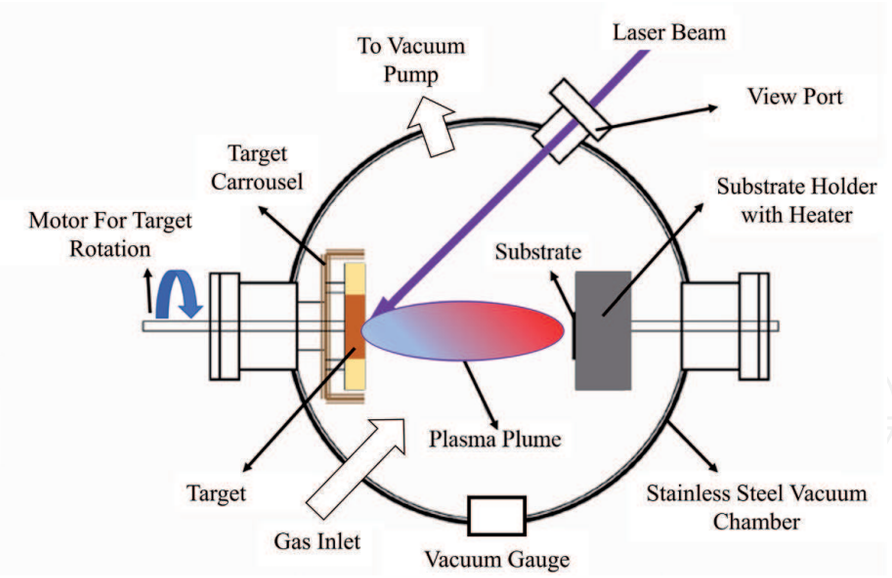

Figure 2.
Schematic view of a typical PLD process. Adapted from Ref. [37].

A typical illustration of a PLD process is shown in **Figure 2**. Compared with the conventional methods discussed above, PLD exhibits the following advantages:

- PLD is the most versatile growth method where a focused and high-energy pulsed laser ionizes almost all types of materials, because of the generation of instantaneous and localized high temperatures up to tens of thousands of ^{O}C on the target's surface. Therefore, majority of the materials can be ablated to form a plasma, which carries out the deposition. In addition, PLD exhibits an excellent compatibility with different substrates which provides numerous routes for the construction of heterojunctions-based devices.

- PLD is highly scalable, because the plasma plume can be readily positioned and directed just by adjusting the external optical path of the laser beam. Consequently, PLD is very much suitable for the growth of wafer-scale and uniform TMDCs for practical industrial production. Serna *et al*. [38] have successfully fabricated continuous bilayers of MoS_2 on sapphire with a diameter up to ~50.8 mm using PLD. Singh *et al*. [39] have also synthesized centimeter-scale MoS_2 thin films on various substrates.

- The substrate temperature required for the PLD growth of TMDCs is relatively low when compared with techniques like CVD and sputtering because the species (atoms, molecules, ions, etc.) ablated by the focused pulsed laser possess a very high energy, and therefore, can freely migrate on the substrate's surface. Therefore, direct growth of TMDCs on substrates that are intolerable towards high temperature can be achieved with PLD. For instance, Singh *et al*. [39] have successfully fabricated MoS_2 on InN at a low substrate temperature of 450°C. It may be noted that low temperature deposition is required for InN as it dissociates above 500°C.

- PLD is a clean, highly efficient, safe, and highly controlled deposition technique where the product is highly continuous and uniform. Due to the ultrahigh vacuum growth conditions, the products of PLD are clean and contamination-free. Furthermore, Siegel *et al*. [32] fabricated MoS_2 on centimeter-scale

sapphire substrates using PLD, varying the thickness from 60 monolayers down to a single monolayer, just by tuning the number of laser pulses.

In the past few years, TMDCs have elicited tremendous research interest, owing to their novel properties in the 2D form, which has triggered a spark in the growth of TMDCs using PLD [18]. In this part of the chapter, a few reports describing the chronological developments in the area of PLD grown TMDCs have been briefly discussed. One of the earliest works on PLD deposited MoS_2 was reported by Zabinski *et al*. [40], where they have prepared PbO-MoS_2 thin films for tribological applications. Other early reports on MoS_2 thin films by PLD include growth of amorphous MoS_2 by McDevitt *et al*. [41] and MoS_2 coatings for friction-related studies by Mosleh *et al*. [42]. The major advancements in this area have been achieved in the past few years. In 2010, Fominski *et al*. [43] have experimentally studied the fabrication of $MoSe_x$ thin films with varying compositions obtained by PLD in vacuum condition and in presence of different rarefied gases. They also developed a process-based mathematical model which played a dominant role on the chemical composition of these thin films. Loh *et al*. [44] in 2014 fabricated MoS_2 on different metals such as Ag, Ni, Al, and Cu by PLD. In 2015, a significant step towards the fabrication of transfer-free TMDC-based PDs was demonstrated by Serrao *et al*. [45] in which MoS_2 was directly deposited on substrates like sapphire, SiC-6H and GaN. The first significant work towards the wafer-scale growth of TMDCs by PLD was done by Siegel *et al*. [32] who reported growth of centimeter-scale MoS_2 thin films of varying thickness (from monolayer to 60 monolayers). Growth of other members of the TMDC family such as WS_2 was also investigated simultaneously. In 2015, Loh *et al*. [46] synthesized WS_2 thin films on Ag substrates by PLD and reported the thickness dependent Raman and PL spectra. However, the obtained WS_2 was having a mixed phase (1T and 2H). In subsequent works, Yao *et al*. [47] obtained the pure 2H phase WS_2 directly by PLD on insulating SiO_2/Si substrates. The growth of selenides via PLD usually suffers from a large number of Se vacancies. Therefore, a two-step growth method was adopted for production of $MoSe_2$ [48]. This included deposition of MoO_3 film via PLD, followed by its selenization. Later on, Mohammed *et al*. [49] achieved 1–8 monolayers of WSe_2 via single-step deposition. This was achieved through a hybrid PLD cluster, where a tungsten target was ablated by the laser beam and selenium vapors were synchronously provided from an effusion cell by thermal evaporation. In 2018, a single-step PLD approach was used by Seo *et al*. [50] to deposit WSe_2 on Al_2O_3 and SiO_2/Si substrates by using a Se-rich target. Lately, Gao *et al*. [51] demonstrated a two-step synthesis route to fabricate 2D WTe_2, which included PLD of amorphous WTe_2 target followed by annealing treatment of the thin films in a Te atmosphere. These reports suggest that the technique of PLD can be suitably applied for the successful production of various TMDCs. In the next section, we will discuss in detail about the fundamentals associated with PLD.

3. Basics of pulsed laser deposition

PLD falls under the category of physical vapor deposition and is a method used to synthesize materials (generally thin films) in an ultrahigh vacuum environment. The development in the field of laser-assisted film growth can be traced back to 1960, after the successful technical realization of the first laser by Maiman [52]. Following on from there, from just being a growth method for fundamental laboratory research, PLD has moved on to become a technique employed in industries. A typical PLD system mainly consists of a laser (usually an excimer laser), an optical path system consisting of apertures, lenses and reflectors, and a stainless-steel

growth chamber equipped with gas paths, vacuum pumps, vacuum gauges, and a heating source [37]. The basic principle behind a PLD process is that a high-intensity pulsed laser interacts with the target or the source material (called ablation) and produces a plasma plume of the target material [37]. The formation of plasma involves a sequence of complex phenomena such as collision, localized heating and subsequent ionization of atoms and molecules. Afterwards, the plasma plume expands, travels downstream, condenses on the substrates and finally crystallizes into the desired materials [37]. **Figure 3** shows the PLD setup located in Materials Research Centre, Indian Institute of Science, Bangalore, India.

The major advantage of a PLD system is that the laser can be operated from outside the vacuum chamber. Thus, just by changing the optical paths of the laser beam, a single laser source can be used for multiple deposition systems. All the other components such as the target carousel, substrate holder, heater, vacuum gauges, and so on are mounted in the vacuum chamber. A set of optical components such as apertures and mirrors are used to focus the pulsed laser beam over the target surface. Therefore, a variety of materials (semiconductors, metals and insulators) can be grown by PLD just by optimizing the growth parameters and by incorporation of different gases during the process in a controlled manner. With this, the exact stoichiometry of the target material can be copied down onto the substrates, which is one of the major benefits of PLD over other deposition techniques. Some of the important parameters associated with PLD have been described below.

Laser source: A krypton fluoride (KrF) laser is a type of excimer laser, and with a wavelength of 248 nm, it is a deep UV laser which is commonly used for the growth of various thin films as the absorption spectrum of most of the inorganic materials lies in the range of 200–400 nm. Typically, excimer lasers contain a mixture of two gases: a noble gas such as argon, xenon or krypton; and a halogen such as chlorine or fluorine. Under suitable conditions of stimulation and pressure, an excimer molecule is created, which decays via a stimulated emission and a coherent beam of stimulated radiation is emitted in the UV range. The continuous emission is

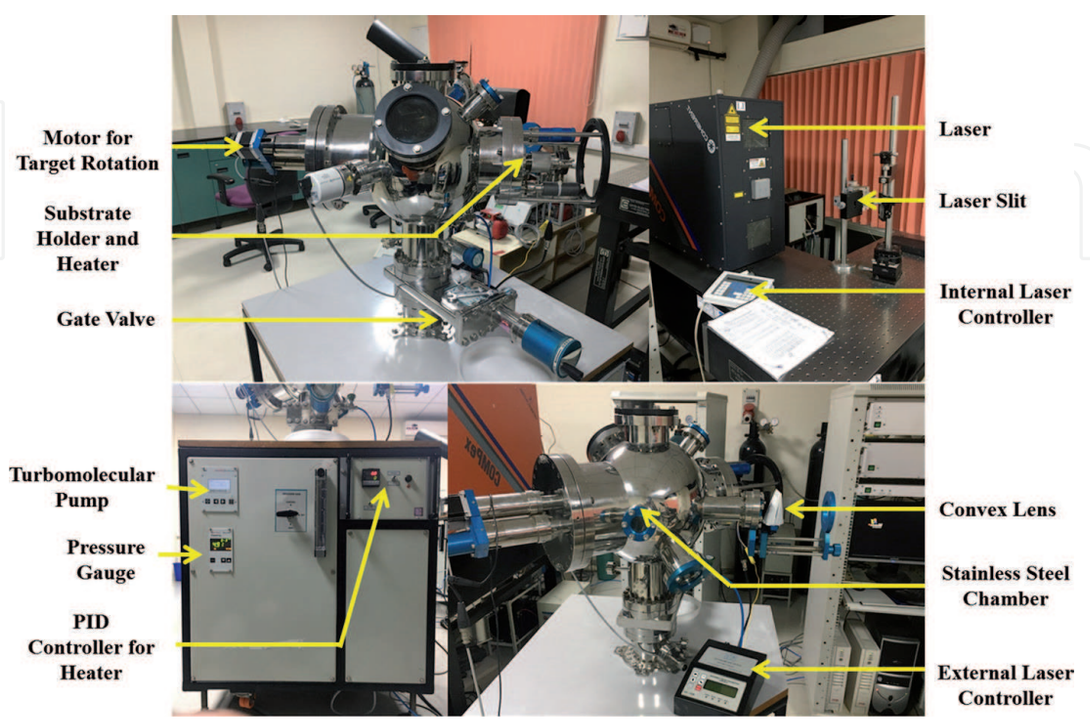

Figure 3.
PLD setup in Materials Research Centre, Indian Institute of Science, Bangalore, India.

then converted into a pulse by various discharge mechanisms and a pulse width of ~10–20 nanoseconds (ns) can be achieved.

Laser fluence: The laser fluence or laser energy density is defined as the laser output energy per unit area and is a very important parameter which decides the proper ablation of the target where the laser beam interacts with the target. A minimum threshold laser fluence is required to carry out the proper ablation process, otherwise, only evaporation takes place. The plume formation depends upon the target conditions such as its density, porosity, morphology, and compositional impurities as well as the laser conditions such as laser pulse duration and laser pulse width. If the laser fluence is much above the threshold value, crystallographic defects and damage can occur in the deposited thin film because of the bombardment by the ablation particles possessing high kinetic energy. Also, it can lead to macroscopic particles ejection during the process of ablation, particulate formation on thin films as well as back-sputtering of species from the deposited thin film. Various mechanisms have been proposed for the formation of particulates and several methods have been devised to minimize these effects [53, 54].

Laser-target interactions: The three main processes taking place during the laser-target interaction are: (i) the laser beam interacts with the surface of the target and gets absorbed into surface layer; (ii) the removal of atomic species from the material is done by vaporization of the surface region in a non-equilibrium state; (iii) afterwards, rapid vaporization further produces a recoil pressure, which leads to the expulsion of the molten pool and produces the plasma plume, and the formed plasma is a collection of electrons, neutral atoms, ions, etc. Therefore, the absorption process is highly dependent on the target properties as well as the laser characteristics. Also, this absorption process is different for metals, insulators and semiconductors [55, 56]. When the laser beam interacts with the target, the photoenergy gets converted into electronic excitations immediately, and the energy relaxation through lattice takes place in ~1 picosecond (ps). Next, the photoenergy is transformed into heat diffusion (over a few microseconds (μs)), which results in the melting of the solid surface (in tens of ns). During the laser-target interactions, the localized temperature of the target reaches up to 10,000 ^{O}C or even higher, leading to the evaporation of the target material. At this point of time, the plume formation takes place (in the range of few μs). The plasma plume consists of atoms, electrons, ions and particulates of varying sizes, ranging from nanometer (nm) to micrometer (μm). This plasma reaches the substrate and undergoes re-solidification and condenses in the form of a thin film [53, 57].

In most of the cases, melting of a material depends on the rate of thermal conduction via lattice, which can be well described by the Fick's laws of diffusion. If the heated volume of the material is smaller than or equivalent to the thickness of ablated layer per laser pulse, then congruent melting will take place. Hence, PLD offers the advantage of congruent melting and vaporization. The amount of heated volume depends on the time of the laser-target interaction, i.e. the pulse duration. For a pulse duration of ~10 ps, heat diffusion will not play a role in the melting and vaporization of the material, whereas, above ~20 ps, conventional heat diffusion dependent ablation occurs [57]. Therefore, the use of a pulsed laser with a pulse duration of a few ns is more likely to provide congruent ablation. This allows the PLD process to preserve the anion-cation stoichiometry of the target material during the mass transfer of the material from the target onto the substrate.

Ambient growth pressure: The background pressure during deposition is a very important and critical parameter that plays a significant role in the plume collisions and plasma dynamics. Keeping the right background pressure is of utmost importance in order to obtain controlled stoichiometric products during the PLD growth. A specific phase and composition of a material can be achieved under controlled

and optimized conditions of background pressure at specific temperature. Plasma species with kinetic energies greater than 50 eV can re-sputter the material already deposited on the substrate and this usually leads to a lower deposition rate, modifications in the stoichiometry of the film, and increase the surface roughness. Controlling the background pressure can reduce re-sputtering of the deposited thin films. Increasing the background gas pressure to an optimum value slows down the highly energetic species in the dilating plasma plume [58].

Target-substrate distance: The target to substrate distance is a useful parameter for reducing the particulate formation since majority of the PLD depositions are carried out in high pressure conditions. If the thin film is deposited in vacuum environment, the target to substrate distance mainly affects the angular spread of the ejected flux. Thus, the effect of target to substrate distance and the background gas pressures is inter-related. The plume length decreases as the ambient gas pressure increases, because of the increased collisions between the plume species and background gas molecules. Therefore, a smaller target to substrate distance should be kept in the case of depositions carried out at high pressures.

Deposition rate: This mainly depends on the repetition rate or the frequency of laser shots which controls the volume or amount of the plume species reaching the substrate and, thus, controls the thickness of the deposited thin film. Deposition rate also depends on the background gas pressure as described previously and mainly modulates the super-saturation process during deposition, which has an influence on the critical nucleation point and the density of nucleation sites. Also, ultra-smooth thin films can be obtained at optimized deposition rates.

Substrate temperature: Substrate temperature plays a critical role in terms of the diffusion barrier during the growth process and strongly affects the growth modes. It influences the nucleation process as well as the mobility of the condensed species across the substrate, and therefore, is crucial in deciding the phase boundary in the crystalline thin films during PLD growth. At lower substrate temperatures, the thin film produced may be amorphous or polycrystalline due to the lower nucleation rate, as the thermal energy provided is too small for overcoming the nucleation barrier. When the substrate temperature is too high, the nucleation rate gets limited due to the high rate of atomic exchange between the solid and gaseous species. Thus, an optimum temperature is required for the easy crystallization of thin films as it becomes easier to overcome the nucleation barrier and form nuclei on the substrate [57].

4. Recent advancements in the PLD growth of TMDCs-based PDs

In general, the PLD-grown TMDCs-based PDs exhibit device performance that is comparable with the PDs based on traditional bulk semiconductors. Additionally, PLD is also beneficial for scalable production up to the wafer-scale. Therefore, growth of these TMDCs through PLD for applications in photodetection shows a tremendous potential to translate the fundamental laboratory research to realization of industrial and practical applications.

MoS_2 is probably the most studied material among various TMDCs and was probably the first member to be fabricated by PLD. One of the earliest investigations on the photodetection studies of MoS_2-based PDs was done by Alkis *et al*. [59], in which the authors have fabricated MoS_2 nanocrystallites through PLD in deionized water and have demonstrated ultraviolet photodetection using the thin films of the obtained MoS_2 nanocrystallites. Mostly, the PLD fabricated PDs based on the TMDCs are in the form of thin films. The earliest MoS_2 thin film-based PD grown by PLD can be traced back to 2014, when Late *et al*. [60] synthesized wafer-scale MoS_2 thin films on flexible

kapton substrates. The devices showed a good photoresponse towards UV light, with stable response and recovery in self-powered mode (**Figure 4a** and **b**). The origination of this self-powered behavior might be from the unintentional inhomogeneities in the contact electrodes [61, 62]. However, the observed response was very weak in the zero-biased mode. This work demonstrated that layered TMDCs can be promising candidates to be used as flexible devices in future photonic applications. In the meantime, researchers across the world started to explore the synthesis of other TMDCs by PLD. In 2015, Yao *et al*. [47] deposited multilayered WS_2 by PLD and performed detailed and systematic investigations on its photodetection properties (**Figure 4c–f**). The synthesized device exhibited a broadband and reproducible photoresponse with good stability. The photoresponse in ambient conditions reached 0.51 AW^{-1}, which was several orders higher than the CVD-grown WS_2 thin films. In vacuum conditions, the responsivity was found to be enhanced to a value of 0.7 AW^{-1}. The lower responsivity in ambient conditions has been explained on the basis of oxygen molecules adsorbed on the surface of WS_2 which trap conduction electrons, and form O_2^-. These species act as recombination centres for the photogenerated carriers. Thus, a greater

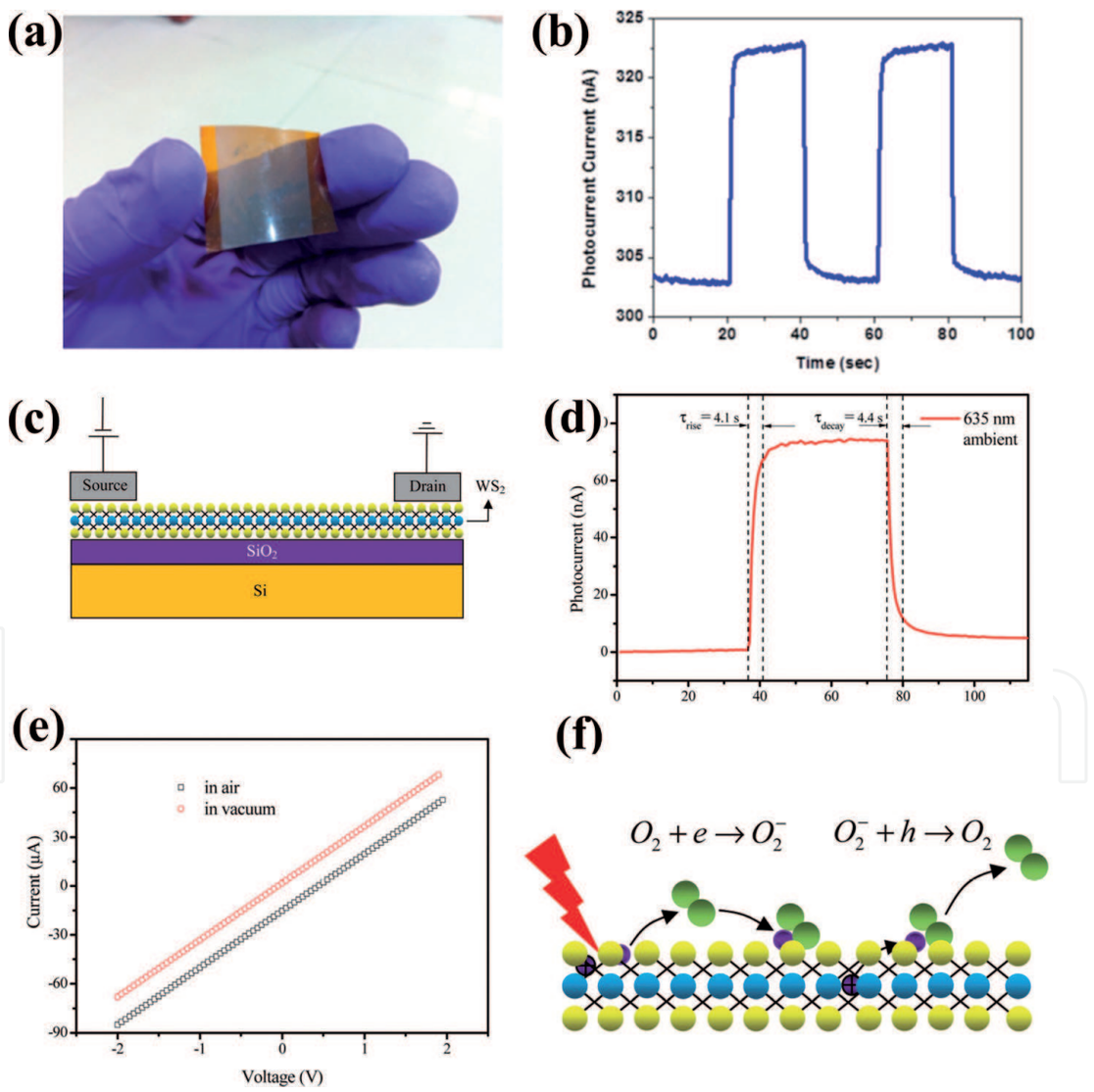

Figure 4.
(a) MoS_2 thin film deposited on flexible kapton substrate and (b) temporal response of the device in zero-bias mode. Figures have been reproduced with permission from Ref. [60]. (c) Cross-sectional schematic view of the WS_2-based photoresistor, (d) temporal response of the device in air, (e) I-V curves of the WS_2-based device in vacuum and in air, and (f) schematic of the photodetection mechanism based on adsorption and desorption of O_2 molecules. Figures have been reproduced with permission from Ref. [47].

number of adsorbed O_2 molecules are present in ambient air environment, which hampers the responsivity of the device. Furthermore, the device maintained a stable and reproducible photoswitching even after one-month of storage in air, indicating the robustness of the device.

The progress in the PLD growth of TMDCs has been quite significant, however, the crystal quality normally remains inferior when compared to the bulk natural crystals. This opens a window to further improve the device quality as well as the performance of PLD-fabricated PDs. One such work has been reported recently, where Wang *et al*. [63] have attained a dramatic improvement in the quality of the PLD-synthesized WS_2 photoresistors by using a post-synthesis annealing procedure. With increase in the post-deposition annealing temperature from 310 to 610°C, the device performance parameters of the WS_2-based PD (annealed at 610°C) enhanced by 2–3 orders of magnitude when compared to the devices annealed at lower temperatures. Annealing treatment usually provides a sufficient amount of energy and time to the atoms and molecules, for the structural reconstruction to annihilate crystal defects, and thus, has been adopted as a universal post-fabrication technique for improving the quality of the products. In another work, Yao *et al*. [64] have synthesized a hybrid $WS_2/Bi_2Te_3/SiO_2/Si$-based PD. The purpose of the insertion of the Bi_2Te_3 layer in between WS_2 and SiO_2 was to passivate the interface. The device demonstrated a stable, reproducible and broadband photoresponse (370 to 1550 nm). Moreover, the device showed a high photoresponsivity of 30.7 AW^{-1} and a pronounced specific detectivity of 2.3×10^{11} Jones with a rise time of 20 ms. The performance of the detector has been attributed to the surface passivation of SiO_2 by the Bi_2Te_3 interfacial layer. SiO_2 surface possess a lot of unscreened dangling bonds. When WS_2 is directly deposited on SiO_2, these bonds can introduce a large density of defects at the bottom of the WS_2 layer, which will act as recombination and scattering centers for the photogenerated charge carriers. With the introduction of Bi_2Te_3 layer, these dangling bonds are greatly suppressed, and this results in the growth of WS_2 film with high crystalline quality, which eventually enhances the PD's performance.

Spectral range of a PD is equally important when compared with the other figures of merit and altering the effective wavelength range of TMDC-based PDs is extremely important for specific applications. It has been shown that by introducing defect states in the forbidden gap of a semiconductor, the detection range can be dramatically extended, and sub-band gap detection can be accomplished. Xie *et al*. [65] have demonstrated ultra-broadband MoS_2-based PDs through PLD by forming sulfur vacancies in MoS_2. The S/Mo atomic ratio was modified from 1.89 to 1.94 by controlling the number of laser pulses from 1200 to 300, resulting in a dramatic increase in the band gap of the semiconductor. Consequently, the S-deficient MoS_2-based PD exhibited an unprecedented ultra-broadband detection range from 445 to 2717 nm. However, theoretical calculations have been done which indicated that the Mo vacancies in MoS_2 possess a higher capability for narrowing the band gap. Therefore, in a subsequent work, Xie *et al*. [66] have synthesized a series of Mo-deficient MoS_2-based PDs by moderating the target to substrate distance during the PLD growth. As a result of these modulations, the effective spectral range of a $MoS_{2.17}$ PD spanned all over from 445 nm to 9536 nm. Although the detection range can be extended up to mid infrared (MIR) with the introduction of the defect states, however, it is accompanied by certain challenges that hinders the usability of this method in practical devices. These include the control over the creation of these defects, which is still an unresolved problem. Furthermore, the electronic properties of the charge carriers are severely hampered owing to the increased scattering effects from these defect states. Thus, such devices often suffer from meager responsivities and slower response speeds.

Recently, Jiao *et al*. [67] have synthesized high-quality and wafer-scale 2D layered MoS_2 thin films by PLD. The device exhibited competitive device performance to the commercial Si and Ge-based PDs. The value of the responsivity was recorded to be 1.96 AW^{-1} for single layer MoS_2-based device, under 300 nm light illumination (**Figure 5**). The PD shows a broadband photoresponse ranging from UV to NIR, with a fast response of 96 ms. This enhancement in the performance was attributed to the variation in the Schottky barrier at the Au/MoS_2 interface.

The above discussed PLD-grown TMDC-based PDs are based on the metal-semiconductor-metal type device configuration, and suffer from relatively lower photoresponsivity, low on/off ratios, narrowband detection and slower detection speed. Hence, strategies are being developed to overcome these limitations. PDs having transparent electrodes such as indium tin oxide (ITO) and graphene, instead of the conventional metal contacts and PDs based on heterojunctions of two or more materials have many advantages such as low value of dark current, higher on/off current ratios, broadband detection range, and higher responsivities due to favorable band alignments.

One such work was carried out in 2016, when Zheng *et al*. [68] successfully prepared centimeter-scale and highly-crystalline WSe_2 thin films on polyimide substrates by the technique of PLD and have fabricated high-performance PDs based on these WSe_2 thin films. They obtained a broadband spectral response, ranging from 370 to 1064 nm. Moreover, a reproducible photoresponsivity approaching up to 0.92 AW^{-1}, an EQE of 180% and a fast response speed of 0.9 s have also been achieved. The PD also exhibited excellent air durability and mechanical flexibility. The enhanced performance has been attributed to the good Ohmic contacts WSe_2 forms with ITO, because of a low mismatch between the work functions of the two materials. Due to the Ohmic contacts, the carriers can be efficiently injected through the ITO electrodes under an applied bias, which will result in generation of a high photocurrent. Ohmic contacts lead to photodetection mechanisms based on the intrinsic properties of the photosensitive material under light irradiation.

Using a similar approach of integration of ITO electrodes on the device, Kumar *et al*. [69] have reported a UV PD which utilizes few layered MoS_2 deposited by PLD. The device shows a high responsivity of 3×10^4 AW^{-1} and detectivity of 1.81×10^{14} Jones, at a nominal voltage of 2 V with fast response time of 32 ms. This performance is better than most of the reported devices based on 2D layered materials. The PD exhibited a very low value of dark current (~10^{-10} A) which is the reason behind such an excellent device performance. This may be

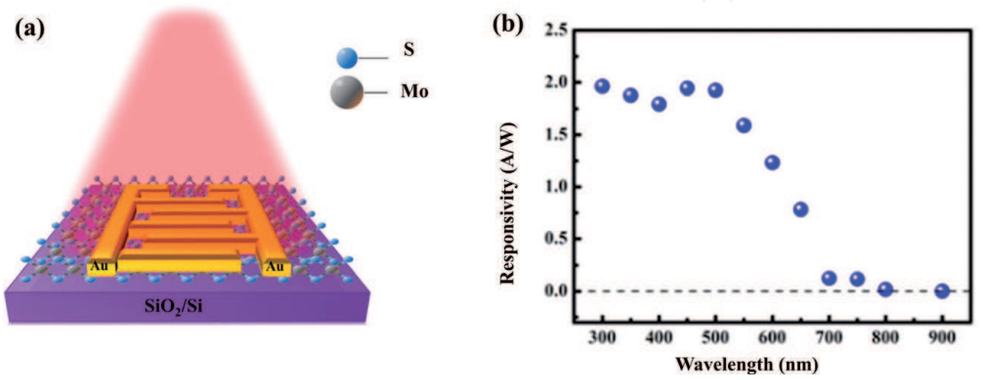

Figure 5.
(a) Schematic of the interdigital patterned gold electrodes to form a metal-semiconductor-metal type contact, and (b) the wavelength dependence of responsivity (300 to 900 nm) for the device. Figures have been reproduced with permission from Ref. [67].

because of suitable band alignment with the ITO electrodes as well as the deposition of high-quality films as the deposition was carried out in the presence of nitrogen gas, leading to lower number of sulfur vacancies.

Till now, all the above reported devices require some external bias for obtaining significant photodetection. Over the years, PDs which consume no external power have attracted a lot of attention because in the current scenario of energy crisis, a lot of research has been focused on energy producing and energy storage devices [70–74]. Such self-powered PDs depend on the interfacial built-in potential which enhances the effective separation of photogenerated carriers. This built-in electric potential also suppresses the dark current, which is another benefit for such PDs. Therefore, these self-powered devices have a great prospect for the next-generation PDs.

In 2015, Yao *et al*. [75] designed a Bi/WS_2/Si heterojunction-based PD by depositing polycrystalline WS_2 and Bi thin films on a p-type Si substrate by PLD (**Figure 6**). The PD exhibited a decent responsivity of 0.42 AW^{-1} and a high detectivity of 1.36 × 10^{13} Jones with ultrahigh sensitivity. It was observed that the performance of the Bi/Si heterointerface was enhanced by the insertion of the WS_2 film. The enhanced device performance has been attributed to the effective passivation of the junction, and enhanced light absorption. Moreover, due to the favorable band alignment, WS_2 acts as a selective carrier blocker, which further enhances the device performance.

Recently, Singh *et al*. [4] demonstrated an MoS_2/AlN/Si-based PD grown by PLD, thus combining the excellent and unique properties of MoS_2 with the matured technologies of Si and III-nitride semiconductors. Moreover, due to a large

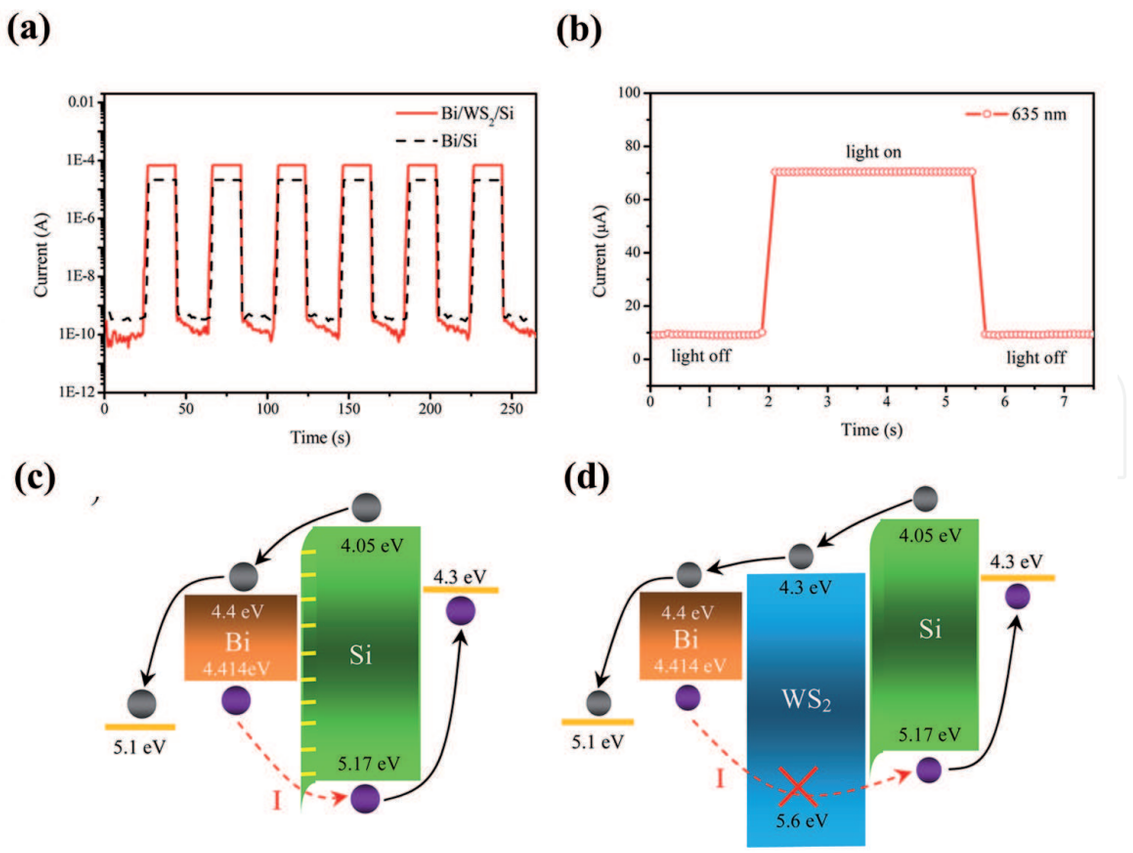

Figure 6.
(a) Transient behavior of the Bi/Si and Bi/WS_2/Si PDs under zero bias. (b) Corresponding single on-off cycle. Schematic of the energy band diagrams of the (c) Bi/Si and (d) Bi/WS_2/Si heterointerfaces. Figures have been reproduced with permission from Ref. [75].

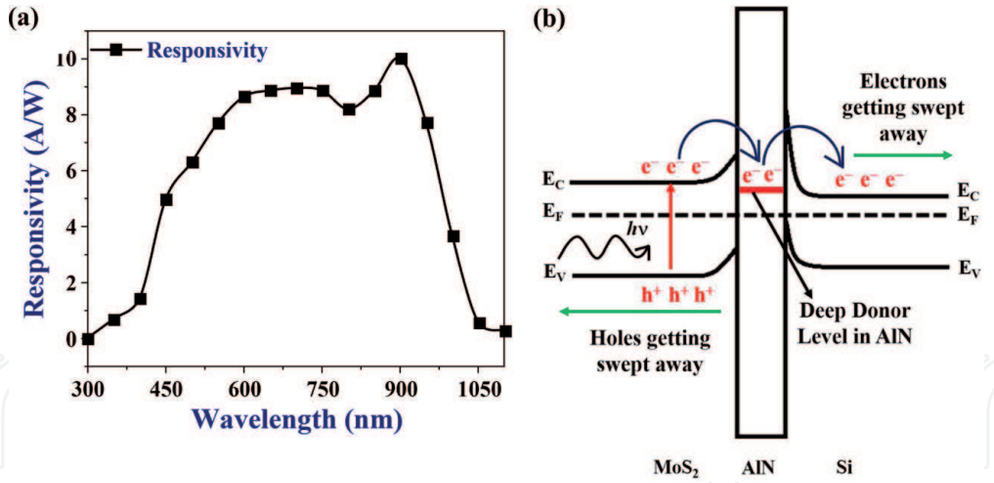

Figure 7.
(a) Spectral response of the MoS_2/AlN/Si-based PD. (b) Schematic of the deep defect states-modulated carrier transport in MoS_2/AlN/Si-based device. Figures have been reproduced with permission from Ref. [4].

difference in the work functions of these materials, the band bending of the heterojunction at the interfaces resulted in self-powered behavior. The vertical transport of the PD exhibited an exceptional broadband photoresponse (300–1100 nm) in the self-powered mode. The device shows a responsivity of 9.93 AW^{-1} under zero-bias condition with ultrafast response speeds (response/recovery times - 12.5/14.9 μs). The photoresponse of MoS_2/Si has also been given, to show the importance of inserting the AlN layer. The MoS_2/Si PD exhibits a responsivity of 1.88 AW^{-1} (~5 times less) in self-powered mode. The authors have shown that the native oxygen defects are present throughout the AlN layer, and this has been confirmed with the help of X-ray photoelectron spectroscopy and transmission electron microscopy. These oxygen impurities form deep donor states in AlN and modulate the transport of the charge carriers, and this leads to the enhanced performance of the MoS_2/AlN/Si-based device (**Figure 7**).

5. Summary

The past few years have undoubtedly witnessed tremendous advances in the PLD growth of TMDCs and their applications in the field of photodetection. In this chapter, the basic properties of TMDCs and the common growth techniques employed for their fabrication have been reviewed briefly, followed by a detailed and elaborated discussion about PLD and the important parameters associated with it. Finally, a progressive investigation about the PDs based on TMDCs fabricated through PLD has been discussed. These extensive achievements in the field of photodetection have unquestionably established PLD as one of the most competitive and reliable methods for fabricating industrial-scale and high-quality TMDCs. PLD, therefore, certainly has a lot of potential to contribute in the development of the next-generation TMDCs-based PDs in the future.

6. Looking into the future

Based on the analysis of the previous reports in this area, an outlook regarding the future of PLD-synthesized TMDCs and the related follow-up research work has been summarized below.

- The research on the PLD-fabricated TMDCs-based PDs is still in its nascent stage and therefore, there is still a room for improvement in the crystal-quality of the PLD-grown thin films, by selecting appropriate substrates and by further tuning and optimizing the various unexplored growth parameters, such as annealing temperature and time, cooling ramp rate, geometry of the laser spot, surface morphology of the source targets, laser frequency, and so on [18].

- Apart from a few reports, most of the research regarding PLD growth of TMDCs for photodetection application is based on the use of a single photosensitive material. Therefore, promising results are expected on the exploration of the heterojunctions of these layered materials with established bulk semiconductors like III-nitrides, which have shown great results in this field. Moreover, TMDCs can serve as excellent substrates for high quality and epitaxial growth of III-nitrides, which would lead to better device performance.

- The use of transparent 2D semiconductors such as graphene or graphene derivatives and semi-metallic phase of TMDCs, can be used in place of the conventional metal electrodes, as they maximize the area of light absorption along with having outstanding electronic properties.

- Till date, researchers and scientists across the world have mostly exploited heterojunctions of TMDCs in their thin film forms. Heterointerfaces based on one dimensional (1D) nanostructures may provide new routes for the development of high-performance devices. The nanowire-based heterostructures of the TMDCs with growth along these nanowires or a core-shell structure will enable a much higher surface to volume ratio and therefore, a larger active interface. This will lead to enhancement in the photoresponse and superior optoelectronic performance.

As a concluding statement, PLD has been proven to be a promising synthesis technique for TMDCs for applications in photodetection, and these PDs have shown outstanding performance that can compete with those of the commercially available PDs. The fabrication through PLD is cost-effective and scalable, and hence, PLD is a perfect tool for fabrication of practical devices for optoelectronic applications at an industrial scale production.

Acknowledgements

D.K.S. is thankful to Council of Scientific and Industrial Research, Government of India, New Delhi for providing senior research fellowship. S.B.K. acknowledges INSA senior scientist fellowship.

IntechOpen

Author details

Deependra Kumar Singh, Karuna Kar Nanda and Saluru Baba Krupanidhi*
Materials Research Centre, Indian Institute of Science, Bangalore, India

*Address all correspondence to: sbkrupanidhi@gmail.com

References

[1] Wu W, Zhang Q, Zhou X, Li L, Su J, Wang F, Zhai T. Self-powered photovoltaic photodetector established on lateral monolayer MoS_2-WS_2 heterostructures. Nano Energy. 2018;51: 45-53.

[2] Singh RK, Kumar J, Kumar A, Kumar V, Kant R, Singh R. Poly(3-hexylthiophene): Functionalized single-walled carbon nanotubes: (6,6)-phenyl-C61-butyric acid methyl ester composites for photovoltaic cell at ambient condition. Solar Energy Materials and Solar Cells. 2010;94(12):2386-94.

[3] Khan MA, Nanda KK, Krupanidhi SB. Mechanistic view on efficient photodetection by solvothermally reduced graphene oxide. Journal of Material Science: Material in Electronics. 2017;28(19):14818-26.

[4] Singh DK, Pant R, Chowdhury AM, Roul B, Nanda KK, Krupanidhi SB. Defect-Mediated Transport in Self-Powered, Broadband, and Ultrafast Photoresponse of a MoS_2/AlN/Si-Based Photodetector. ACS Applied Electronic Materials. 2020;2(4):944-53.

[5] Lopez-Sanchez O, Lembke D, Kayci M, Radenovic A, Kis A. Ultrasensitive photodetectors based on monolayer MoS_2. Nature Nanotechnology. 2013;8(7):497-501.

[6] Pant RK, Singh DK, Roul B, Chowdhury AM, Chandan G, Nanda KK, et al. Photodetection Properties of Nonpolar a-Plane GaN Grown by Three Approaches Using Plasma-Assisted Molecular Beam Epitaxy. physica status solidi (a). 2019;216(18):1900171.

[7] Sai Manohar GV, Krupanidhi SB, Nanda KK. Giant enhancement in photoresponse via engineering of photo-induced charge (electron and hole) transfer in linear and non-linear devices. Sensors and Actuators A: Physical. 2020;304:111842.

[8] Chowdhury AM, Chandan G, Pant R, Roul B, Singh DK, Nanda KK, et al. Self-Powered, Broad Band, and Ultrafast InGaN-Based Photodetector. ACS Applied Material & Interfaces. 2019;11(10):10418-25.

[9] Hsu L-H, Kuo C-T, Huang J-K, Hsu S-C, Lee H-Y, Kuo H-C, et al. InN-based heterojunction photodetector with extended infrared response. Optical Express. 2015;23(24):31150.

[10] Arora K, Kumar M. Sputtered-Growth of High-Temperature Seed-Layer Assisted β-Ga_2O_3 Thin Film on Silicon-Substrate for Cost-Effective Solar-Blind Photodetector Application. ECS Journal of Solid State Science and Technology. 2020;9(6):065013.

[11] Arora K, Singh DP, Fischer P, Kumar M. Spectrally Selective and Highly Sensitive UV Photodetection with UV-A,C Band Specific Polarity Switching in Silver Plasmonic Nanoparticle Enhanced Gallium Oxide Thin-Film. Advanced Optical Materials. 2020;8(16):2000212.

[12] Peytavit E, Arscott S, Lippens D, Mouret G, Matton S, Masselin P, et al. Terahertz frequency difference from vertically integrated low-temperature-grown GaAs photodetector. Applied Physics Letters. 2002;81(7):1174-6.

[13] Berencén Y, Prucnal S, Liu F, Skorupa I, Hübner R, Rebohle L, et al. Room-temperature short-wavelength infrared Si photodetector. Scientific Reports. 2017;7(1):43688.

[14] Monroy E, Calle F, Pau JL, Muñoz E, Omnès F, Beaumont B, et al. AlGaN-based UV photodetectors. Journal of Crystal Growth. 2001;230(3-4):537-43.

[15] Masini G, Cencelli V, Colace L, DeNotaristefani F, Assanto G. A germanium photodetector array for the near infrared monolithically integrated with silicon CMOS readout electronics. Physica E: Low-dimensional Systems and Nanostructures. 2003;16(3-4):614-9.

[16] Zhou YD, Becker CR, Selamet Y, Chang Y, Ashokan R, Boreiko RT, et al. Far-infrared detector based on HgTe/HgCdTe superlattices. Journal of Electronic Materials. 2003;32(7):608-14.

[17] Bowers JE, Srivastava AK, Burrus CA, DeWinter MA, Pollack MA, Zyskind JL. High-speed GaInAsSb/GaSb PIN photodetectors for wavelengths to 2.3 μm. Electronics Letters. 1986;22(3):137-8.

[18] Yao JD, Zheng ZQ, Yang GW. Production of large-area 2D materials for high-performance photodetectors by pulsed-laser deposition. Progress in Materials Science. 2019;106:100573.

[19] Novoselov KS, Geim AK, Morozov SV, Jiang D, Zhang Y, Dubonos SV, et al. Electric field effect in atomically thin carbon films. Science. 2004;306(5696):666-9.

[20] Thakur MK, Gupta A, Ghosh S, Chattopadhyay S. Graphene-Conjugated Upconversion Nanoparticles as Fluorescence-Tuned Photothermal Nanoheaters for Desalination. ACS Applied Nano Materials. 2019;2(4):2250-9.

[21] Thakur MK, Fang C-Y, Yang Y-T, Effendi TA, Roy PK, Chen R-S, et al. Microplasma-Enabled Graphene Quantum Dot-Wrapped Gold Nanoparticles with Synergistic Enhancement for Broad Band Photodetection. ACS Applied Mater & Interfaces. 2020;12(25):28550-60.

[22] Thakur MK, Gupta A, Fakhri MY, Chen RS, Wu CT, Lin KH, et al. Optically coupled engineered upconversion nanoparticles and graphene for a high responsivity broadband photodetector. Nanoscale. 2019;11(19):9716-25.

[23] Liu HF, Wong SL, Chi DZ. CVD Growth of MoS_2-based Two-dimensional Materials. Chemical Vapor Deposition. 2015;21(10-11-12):241-59.

[24] Gonzalez JM, Oleynik II. Layer-dependent properties of SnS_2 and $SnSe_2$ two-dimensional materials. Physical Review B. 2016;94(12):125443.

[25] Lin Y-M, Dimitrakopoulos C, Jenkins KA, Farmer DB, Chiu H-Y, Grill A, et al. 100-GHz Transistors from Wafer-Scale Epitaxial Graphene. Science. 2010;327(5966):662-662.

[26] Li C, Yan X, Song X, Bao W, Ding S, Zhang DW, et al. WSe_2/MoS_2 and $MoTe_2/SnSe_2$ van der Waals heterostructure transistors with different band alignment. Nanotechnology. 2017;28(41):415201.

[27] Nam S-G, Cho Y, Lee M-H, Shin KW, Kim C, Yang K, et al. Barrier height control in metal/silicon contacts with atomically thin MoS_2 and WS_2 interfacial layers. 2D Materials. 2018;5(4):041004.

[28] Ko PJ, Abderrahmane A, Kim N, Sandhu A. High-performance near-infrared photodetector based on nano-layered $MoSe_2$. Semiconductor Science and Technology. 2017;32(6):065015.

[29] Yin Z, Li H, Li H, Jiang L, Shi Y, Sun Y, et al. Single-Layer MoS_2 Phototransistors. ACS Nano. 2012;6(1):74-80.

[30] Zhuo R, Wang Y, Wu D, Lou Z, Shi Z, Xu T, et al. High-performance self-powered deep ultraviolet photodetector based on MoS_2/GaN p–n heterojunction. Journal of Materials Chemistry C. 2018;6(2):299-303.

[31] Kang M-A, Kim S, Jeon I-S, Lim YR, Park C-Y, Song W, et al. Highly efficient and flexible photodetector based on MoS_2–ZnO heterostructures. RSC Advances. 2019;9(34):19707-11.

[32] Siegel G, Venkata Subbaiah YP, Prestgard MC, Tiwari A. Growth of centimeter-scale atomically thin MoS_2 films by pulsed laser deposition. APL Materials. 2015;3(5):056103.

[33] Manzeli S, Ovchinnikov D, Pasquier D, Yazyev OV, Kis A. 2D transition metal dichalcogenides. Nature Reviews Materials. 2017;2(8):17033.

[34] Splendiani A, Sun L, Zhang Y, Li T, Kim J, Chim C-Y, et al. Emerging Photoluminescence in Monolayer MoS_2. Nano Letters. 2010;10(4):1271-5.

[35] Singh A, Singh AK. Origin of n -type conductivity of monolayer MoS_2. Physical Review B. 2019;99(12):121201.

[36] Tangi M, Mishra P, Ng TK, Hedhili MN, Janjua B, Alias MS, et al. Determination of band offsets at GaN/single-layer MoS_2 heterojunction. Applied Physics Letters. 2016;109(3):032104.

[37] Pulsed Laser Deposition (PLD). https://vaccoat.com/blog/pulsed-laser-deposition-pld/.

[38] Serna MI, Yoo SH, Moreno S, Xi Y, Oviedo JP, Choi H, et al. Large-Area Deposition of MoS_2 by Pulsed Laser Deposition with *In Situ* Thickness Control. ACS Nano. 2016;10(6):6054-61.

[39] Singh DK, Roul B, Pant R, Chowdhury AM, Nanda KK, Krupanidhi SB. Different types of band alignment at MoS_2/(Al, Ga, In) N heterointerfaces. Appl Phys Lett. 2020;116(25):252102.

[40] Zabinski JS, Donley MS, Dyhouse VJ, McDevitt NT. Chemical and tribological characterization of PbO:MoS_2 films grown by pulsed laser deposition. Thin Solid Films. 1992;214(2):156-63.

[41] McDevitt NT, Bultman JE, Zabinski JS. Study of Amorphous MoS_2 Films Grown by Pulsed Laser Deposition. Applied spectroscopy. 1998;52(9):1160-4.

[42] Mosleh M, Laube SJP, Suh NP. Friction of Undulated Surfaces Coated with MoS_2 by Pulsed Laser Deposition. Tribology Transactions. 1999;42(3):495-502.

[43] Fominski VYu, Romanov RI, Gnedovets AG, Nevolin VN. Formation of the chemical composition of transition metal dichalcogenide thin films at pulsed laser deposition. Technical Physics. 2010;55(10):1509-16.

[44] Loh TAJ, Chua DHC. Growth Mechanism of Pulsed Laser Fabricated Few-Layer MoS_2 on Metal Substrates. ACS Applied Materials & Interfaces. 2014;6(18):15966-71.

[45] Serrao CR, Diamond AM, Hsu S-L, You L, Gadgil S, Clarkson J, et al. Highly crystalline MoS_2 thin films grown by pulsed laser deposition. Applied Physics Letters. 2015;106(5):052101.

[46] Loh TAJ, Chua DHC, Wee ATS. One-step Synthesis of Few-layer WS_2 by Pulsed Laser Deposition. Scientific Reports. 2016;5(1):18116.

[47] Yao JD, Zheng ZQ, Shao JM, Yang GW. Stable, highly-responsive and broadband photodetection based on large-area multilayered WS_2 films grown by pulsed-laser deposition. Nanoscale. 2015;7(36):14974-81.

[48] Ullah F, Nguyen TK, Le CT, Kim YS. Pulsed laser deposition assisted grown continuous monolayer $MoSe_2$. CrystEngComm. 2016;18(37):6992-6.

[49] Mohammed A, Nakamura H, Wochner P, Ibrahimkutty S, Schulz A,

Müller K, et al. Pulsed laser deposition for the synthesis of monolayer WSe_2. Applied Physics Letters. 2017;111(7):073101.

[50] Seo S, Choi H, Kim SY, Lee J, Kim K, Yoon S, et al. Growth of Centimeter-Scale Monolayer and Few-Layer WSe_2 Thin Films on SiO_2/Si Substrate via Pulsed Laser Deposition. Advanced Materials Interfaces. 2018;5(20):1800524.

[51] Gao M, Zhang M, Niu W, Chen Y, Gu M, Wang H, et al. Tuning the transport behavior of centimeter-scale WTe_2 ultrathin films fabricated by pulsed laser deposition. Applied Physics Letters. 2017;111(3):031906.

[52] Maiman TH. Ruby laser systems. United States patent, US 3,353,115. 1967.

[53] Stafe M, Marcu A, Puscas NN. Pulsed Laser Ablation of Solids - Basics, Theory and Applications. Springer Series in Surface Sciences; 2014.

[54] Eason R. Pulsed laser deposition of thin films: applications-led growth of functional materials. John Wiley & Sons; 2007.

[55] Singh RK, Narayan J. A novel method for simulating laser-solid interactions in semiconductors and layered structures. Materials Science and Engineering: B. 1989;3(3):217-30.

[56] Wood RF, Giles GE. Macroscopic theory of pulsed-laser annealing. I. Thermal transport and melting. Physical Review B. 1981;23(6):2923-42.

[57] Daramalla, V. Titanium Niobium complex oxide ($TiNb_2O_7$) thin films for micro battery applications. PhD thesis. Indian Institute of Science, Bangalore; 2015.

[58] Gai Z, Kalinin SV, Li A-P, Shen J, Baddorf AP. In Situ Observations and Tuning of Physical and Chemical Phenomena on the Surfaces of Strongly Correlated Oxides. Advanced Functional Materials. 2013;23(20):2477-89.

[59] Alkis S, Öztaş T, Aygün LE, Bozkurt F, Okyay AK, Ortaç B. Thin film MoS_2 nanocrystal based ultraviolet photodetector. Optics Express. 2012;20(19):21815.

[60] Late DJ, Shaikh PA, Khare R, Kashid RV, Chaudhary M, More MA, et al. Pulsed Laser-Deposited MoS_2 Thin Films on W and Si: Field Emission and Photoresponse Studies. ACS Applied Materials & Interfaces. 2014;6(18):15881-8.

[61] Pant R, Singh DK, Chowdhury AM, Roul B, Nanda KK, Krupanidhi SB. Highly Responsive, Self-Powered *a*-GaN Based UV-A Photodetectors Driven by Unintentional Asymmetrical Electrodes. ACS Applied Electronic Materials. 2020;2(3):769-79.

[62] Rambabu A, Singh DK, Pant R, Nanda KK, Krupanidhi SB. Self-powered, ultrasensitive, room temperature humidity sensors using SnS_2 nanofilms. Scientific Reports. 2020;10(1):14611.

[63] Wang H, Ng SM, Wong HF, Wong WC, Lam KK, Liu YK, et al. Effect of post-annealing on laser-ablation deposited WS_2 thin films. Vacuum. 2018;152:239-42.

[64] Yao J, Zheng Z, Yang G. Layered-material WS_2/topological insulator Bi_2Te_3 heterostructure photodetector with ultrahigh responsivity in the range from 370 to 1550 nm. Journal of Materials Chemistry C. 2016;4(33):7831-40.

[65] Xie Y, Zhang B, Wang S, Wang D, Wang A, Wang Z, et al. Ultrabroadband MoS_2 Photodetector with Spectral Response from 445 to 2717 nm. Advanced Materials. 2017;29(17):1605972.

[66] Xie Y, Liang F, Wang D, Chi S, Yu H, Lin Z, et al. Room-Temperature Ultrabroadband Photodetection with MoS_2 by Electronic-Structure Engineering Strategy. Advanced Materials. 2018;30(50):1804858.

[67] Jiao L, Jie W, Yang Z, Wang Y, Chen Z, Zhang X, et al. Layer-dependent photoresponse of 2D MoS_2 films prepared by pulsed laser deposition. Journal of Materials Chemistry C. 2019;7(9):2522-9.

[68] Zheng Z, Zhang T, Yao J, Zhang Y, Xu J, Yang G. Flexible, transparent and ultra-broadband photodetector based on large-area WSe_2 film for wearable devices. Nanotechnology. 2016;27(22):225501.

[69] Kumar S, Sharma A, Ho YT, Pandey A, Tomar M, Kapoor AK, et al. High performance UV photodetector based on MoS_2 layers grown by pulsed laser deposition technique. Journal of Alloys and Compounds. 2020;835:155222.

[70] Shi D, Wang G, Li C, Shen X, Nie Q. Preparation and thermoelectric properties of $MoTe_2$ thin films by magnetron co-sputtering. Vacuum. 2017;138:101-4.

[71] Kumar A, Singh RK, Singh HK, Srivastava P, Singh R. Enhanced capacitance and stability of p-toluenesulfonate doped polypyrrole/carbon composite for electrode application in electrochemical capacitors. Journal of Power Sources. 2014;246:800-7.

[72] Kumar S, Chaudhary D, Khare N. Enhanced thermoelectric figure of merit in Bi_2Te_3–CNT–PEDOT nanocomposite by introducing conducting interfaces in Bi_2Te_3 nanostructures. APL Materials. 2019;7(8):081123.

[73] Kumar A, Singh RK, Singh HK, Srivastava P, Singh R. Mechanism of direct current electrical charge conduction in *p*-toluenesulfonate doped polypyrrole/carbon composites. Journal of Applied Physics. 2014;115(10):103702.

[74] Kumar A, Singh HK, Singh RK, Singh R, Srivastava P. P-toluenesulfonate doped polypyrrole/carbon composite electrode and a process for the preparation thereof. United States patent US 10,074,453. 2018.

[75] Yao J, Zheng Z, Shao J, Yang G. Promoting Photosensitivity and Detectivity of the Bi/Si Heterojunction Photodetector by Inserting a WS_2 Layer. ACS Applied Materials & Interfaces. 2015;7(48):26701-8.